AJNR

Application of 3D Fast Spin-Echo T1 Black-Blood Imaging in the Diagnosis and Prognostic Prediction of Patients with Leptomeningeal Carcinomatosis

J. Oh, S.H. Choi, E. Lee, D.J. Shin, S.W. Jo, R.-E. Yoo, K.M. Kang, T.J. Yun, J.-h. Kim and C.-H. Sohn

AJNR Am J Neuroradiol 2018, 39 (8) 1453-1459
doi: https://doi.org/10.3174/ajnr.A5721
http://www.ajnr.org/content/39/8/1453

Application of 3D Fast Spin-Echo T1 Black-Blood Imaging in the Diagnosis and Prognostic Prediction of Patients with Leptomeningeal Carcinomatosis

J. Oh, S.H. Choi, E. Lee, D.J. Shin, S.W. Jo, R.-E. Yoo, K.M. Kang, T.J. Yun, J.-h. Kim, and C.-H. Sohn

ABSTRACT

BACKGROUND AND PURPOSE: Contrast-enhanced 3D fast spin-echo T1 black-blood imaging selectively suppresses the signal of blood flow and could provide a higher contrast-to-noise ratio compared with contrast-enhanced 3D ultrafast gradient recalled echo (contrast-enhanced gradient recalled echo) and 2D spin-echo T1WI (contrast-enhanced spin-echo). The purpose of our study was to evaluate whether black-blood imaging can improve the diagnostic accuracy for leptomeningeal carcinomatosis compared with contrast-enhanced gradient recalled-echo and contrast-enhanced spin-echo and, furthermore, to determine whether the grade of leptomeningeal carcinomatosis evaluated on black-blood imaging is a significant predictor of progression-free survival.

MATERIALS AND METHODS: Leptomeningeal carcinomatosis ($n = 78$) and healthy ($n = 31$) groups were enrolled. Contrast-enhanced gradient recalled-echo, contrast-enhanced spin-echo, and black-blood imaging were separately reviewed, and a diagnostic rating (positive, indeterminate, or negative) and grading of leptomeningeal carcinomatosis were assigned. The diagnostic accuracies of the 3 imaging sequences were compared in terms of leptomeningeal carcinomatosis detection. The Kaplan-Meier and the Cox proportional hazards model analyses were performed to determine the relationship between the leptomeningeal carcinomatosis grade evaluated on black-blood imaging and progression-free survival.

RESULTS: Black-blood imaging showed a significantly higher sensitivity (97.43%) than contrast-enhanced gradient recalled-echo (64.1%) and contrast-enhanced spin-echo (66.67%) ($P < .05$). In terms of specificities, we did not find any significant differences among contrast-enhanced gradient recalled-echo (90.32%), contrast-enhanced spin-echo (90.32%), and black-blood imaging (96.77%) ($P > .05$). A Cox proportional hazards model identified the time to metastasis, Karnofsky Performance Scale status, and a combination of the leptomeningeal carcinomatosis grade with a linear pattern as independent predictors of progression-free survival ($P < .05$).

CONCLUSIONS: Black-blood imaging can improve the diagnostic accuracy and predict progression-free survival in patients with leptomeningeal carcinomatosis.

ABBREVIATIONS: CE = contrast-enhanced; GRE = gradient recalled-echo; ICC = intraclass correlation coefficient; KPS = Karnofsky Performance Scale; LC = leptomeningeal carcinomatosis; PFS = progression-free survival; SE = spin-echo

Leptomeningeal carcinomatosis (LC) is a devastating complication of systemic cancer that occurs in approximately 5%–10% of patients with solid tumors and is most commonly observed in patients with breast cancer, lung cancer, or melanoma.[1]

Recently, the incidence of LC has gradually started increasing as the diagnostic rate of primary cancer has increased and the outcome of primary cancer has improved due to effective antineoplastic treatments.[2,3] However, the prognosis for patients with LC is extremely poor, and the median survival rate is 4–6 weeks if not treated, which can be increased to 4–6 months after active treatment with chemotherapy or radiation therapy.[4,5] In addition,

Received February 18, 2018; accepted after revision May 23.

From the Department of Radiology (J.O., S.H.C., E.L., D.J.S., S.W.J., R.-E.Y., K.M.K., T.J.Y., J.-h.K., C.-H.S.), Seoul National University Hospital, Seoul, Korea; Department of Radiology (J.O., S.H.C., R.-E.Y., K.M.K., T.J.Y., J.-h.K., C.-H.S.), Seoul National University College of Medicine, Seoul, Korea; Institute of Radiation Medicine (S.H.C.), Seoul National University Medical Research Center, Seoul, Korea; and Center for Nanoparticle Research (S.H.C.), Institute for Basic Science, Seoul, Republic of Korea.

This study was supported by a grant from the Korea Healthcare Technology R&D Projects, Ministry for Health, Welfare & Family Affairs (HI16C1111); the Brain Research Program through the National Research Foundation of Korea funded by the Ministry of Science, ICT & Future Planning (2016M3C7A1914002); the Basic Science Research Program through the National Research Foundation of Korea funded by the Ministry of Science, ICT & Future Planning (2017R1A2B2006526); Creative-Pioneering Researchers Program through Seoul National University; and Project Code (IBS-R006-D1).

Please address correspondences to Seung Hong Choi, MD, PhD, Department of Radiology, Seoul National University Hospital, 101 Daehak-ro, Jongno-gu, Seoul, 110-744, Republic of Korea; e-mail: verocay@snuh.org

Indicates open access to non-subscribers at www.ajnr.org

Indicates article with supplemental on-line tables.

http://dx.doi.org/10.3174/ajnr.A5721

proper treatment can prevent the deterioration of neurologic symptoms that impair the patient's quality of life.[1,6] Therefore, early diagnosis and proper treatment of LC are the most important strategies to improve the overall survival and quality of life of patients with LC.

However, the diagnosis of LC is still a challenge. Identification of malignant cells by CSF cytology has been the diagnostic criterion standard, but the sensitivity of CSF cytology is limited. The initial cytology is falsely negative in up to 40%–50% of patients with pathologically proved LC, and this measure demonstrates a sensitivity of approximately 75% on repeat spinal tapping.[7,8] With improved visualization of the subarachnoid space, MR imaging, especially contrast-enhanced (CE) T1-weighted imaging, is regarded as a reliable technique for confirming this diagnosis and for assessing the extent of the lesion and its response to therapy.[9,10] However, LC is often missed on MR imaging because the leptomeninx is an anatomically thin membrane and subtle contrast enhancement is often mistaken for blood vessels by readers.

A recently introduced 3D fast spin-echo T1 black-blood imaging is one of the 3D spin-echo sequences that nullifies signals from moving flows[11,12]; in other words, it selectively suppresses the signal of blood flow and provides a higher contrast-to-noise ratio. Several studies have demonstrated that black-blood imaging can improve the diagnostic accuracy of small brain parenchymal metastases due to its higher contrast-to-noise ratio.[13,14] However, there are few studies that have explored the value of black-blood imaging in the detection of LC, and we hypothesized that black-blood imaging has a better diagnostic accuracy in detecting LC than CE 3D ultrafast gradient recalled-echo (CE GRE) and 2D spin-echo T1WI (CE SE).

Therefore, the purpose of our study was to evaluate whether black-blood imaging can improve the diagnostic accuracy for LC proved pathologically or clinically by comparing it with CE GRE and CE SE and, furthermore, to determine whether the grade of LC evaluated on black-blood imaging is a significant predictor of the patient's performance status and progression-free survival (PFS).

MATERIALS AND METHODS

Patients

This retrospective study was approved by the Seoul National University Hospital Institutional Review Board (SNUH IRB) with a waiver of informed consent. From January 2014 to October 2016, MR imaging was performed in 1758 consecutive patients (older than 18 years of age), including black-blood imaging, CE GRE, and CE SE. Among them, 78 patients met the following inclusion criteria: 1) having been diagnosed with LC and meeting the criteria below; 2) having contrast MR images of the brain, including black-blood imaging, CE GRE, and CE SE; and 3) having at least a 3-month follow-up if no progression. The exclusion criteria were as follows: 1) patients with prior intrathecal chemotherapy or whole-brain radiation therapy; and 2) patients with imaging studies from outside institutions or inadequate MR images for the analysis because of motion artifacts. The mean age of the patients was 56.5 years (age range, 19–87 years; 48 female and 30 male patients). The diagnoses were lung cancer (n = 51 patients), breast cancer (n = 19 patients), gastric cancer (n = 5 patients), gallbladder cancer (n = 1 patient), cholangiocarcinoma (n = 1 patient), and osteosarcoma (n = 1 patient).

Table 1: Clinical characteristics

	LC+ (n = 78)	LC− (n = 31)
Age (yr)		
Mean	56.50 ± 13.61	64.03 ± 11.69
Sex (No.) (%)		
Male	30 (38.46%)	19 (61.29%)
Female	48 (61.54%)	12 (38.71%)
Primary cancer (No.) (%)		
Lung cancer	51 (65.38%)	28 (90.32%)
Breast cancer	19 (24.36%)	3 (9.68%)
Other	8 (10.26%)	0
Brain metastasis (No.) (%)		
Yes	60 (76.92%)	0
No	18 (23.08%)	31 (100%)
Extracranial metastasis (No.) (%)		
Yes	48 (61.54%)	1 (3.23%)
No	30 (38.46%)	30 (96.77%)
Neurologic symptom (No.) (%)		
Yes	73 (93.59%)	0
No	5 (6.41%)	31 (100%)
KPS		
Mean	52.56 ± 19.03	80.97 ± 3.01

Note:—LC + indicates patients with leptomeningeal carcinomatosis; LC −, patients without leptomeningeal carcinomatosis.

In addition, 31 patients without LC were also enrolled. We considered LC to be absent if there was no clinical evidence of LC with a follow-up of >12 months, in addition, negative cytology if CSF cytology was performed.[15] The clinical criteria called for no new or progressive neurologic deficits for >12 months after the MR imaging. Only the negative CSF cytology criterion is not adequate because even three separate lumbar punctures can have a false negative rate of >10%.[7,8]

Diagnosis of LC

The diagnosis was made in 1 of 2 ways: (1) a CSF cytology positive for malignant cells, which was repeated up to three times or (2) MRI scans showing LC on both initial and 2–3 month follow-up studies in patients with suspicious cytology (atypical cells) or biochemical test (elevated protein level and/or decreased glucose level in CSF).[1,7,8,10,16-19] The various MR imaging findings used for the diagnosis included superficial sulcal/cisternal enhancement, sulcal/cisternal obliteration, multiple tiny superficial nodules along the sulci/cistern, enhancement of cranial nerves, and hydrocephalus.[7,10] LC may grow in a linear pattern, creating a thin layer of cells spread diffusely over the brain surfaces, or in a nodular growth pattern, involving the leptomeninges in a multifocal skip pattern with intervening tumor-free areas.[4,20]

MR Imaging Acquisition

In this study, MR imaging examinations were performed on 1 of three 3T MR imaging systems with 32-channel head coils, which included Verio (Siemens, Erlangen, Germany), Achieva dStream (Philips Healthcare, Best, the Netherlands), and Discovery MR750w (GE Healthcare, Milwaukee, Wisconsin) scanners. Each MR imaging scanning session included CE GRE, CE SE, and black-blood imaging, sequentially. CE T1WI was obtained after the intravenous administration (manual injection) of gadobutrol

(Gadovist; Bayer Schering Pharma, Berlin, Germany) at a dose of 0.1 mmol/kg of body weight.

The study was conducted in 63, 27, and 19 of 109 patients using the Verio, Achieva dStream, and Discovery MR750w scanners, respectively. The parameters used in the MR imaging examinations are summarized in On-line Table 1.

Image Analysis

A senior neuroradiologist (17 years of brain MR imaging experience) who was blinded to clinical information reviewed the images from each sequence individually and separately and assigned a diagnostic rating (positive, indeterminate, or negative) and a grading of LC. We also scored leptomeningeal enhancement on MR imaging on a 0–5 scale. For each of the cerebral hemispheres, the presence of leptomeningeal enhancement was scored as 0 (absent), 1 (in 1 lobe), or 2 (>1 lobe). For the infratentorial area, it was scored as 0 (absent) or 1 (present).[19] In addition, other imaging parameters were also collected, including the presence and number of brain metastases, the presence of hydrocephalus, the pattern of LC (linear or nodular), and the location of LC in the brain.

For the analysis of the interobserver agreement, 4 neuroradiologists (with 6, 8, 9, and 17 years of neuroimaging experience) who were blinded to clinical information analyzed 109 sets of MR images from each sequence individually and separately and assigned a diagnostic rating (positive, indeterminate, or negative) to each location of the cerebral hemispheres and a grading of LC.

Table 2: Results of the MR imaging readings in cases positive for LC ($n = 78$)

Findings	Imaging Technique		
	CE GRE	CE SE	Black-Blood Imaging
Positive	50	52	76
Indeterminate	7	5	0
Negative	21	21	2
Sensitivity (%)	64.1	66.67	97.43

Note:—Black-blood imaging indicates 3D fast SE T1 black-blood imaging.

Clinical Variables and Follow-Up

The patients' medical records were reviewed, and demographic and clinical data were collected, including age, sex, date of initial cancer diagnosis, date of LC diagnosis, Karnofsky Performance Scale (KPS) score at LC diagnosis, primary cancer histology, history of intrathecal chemotherapy or radiation to the brain, initial

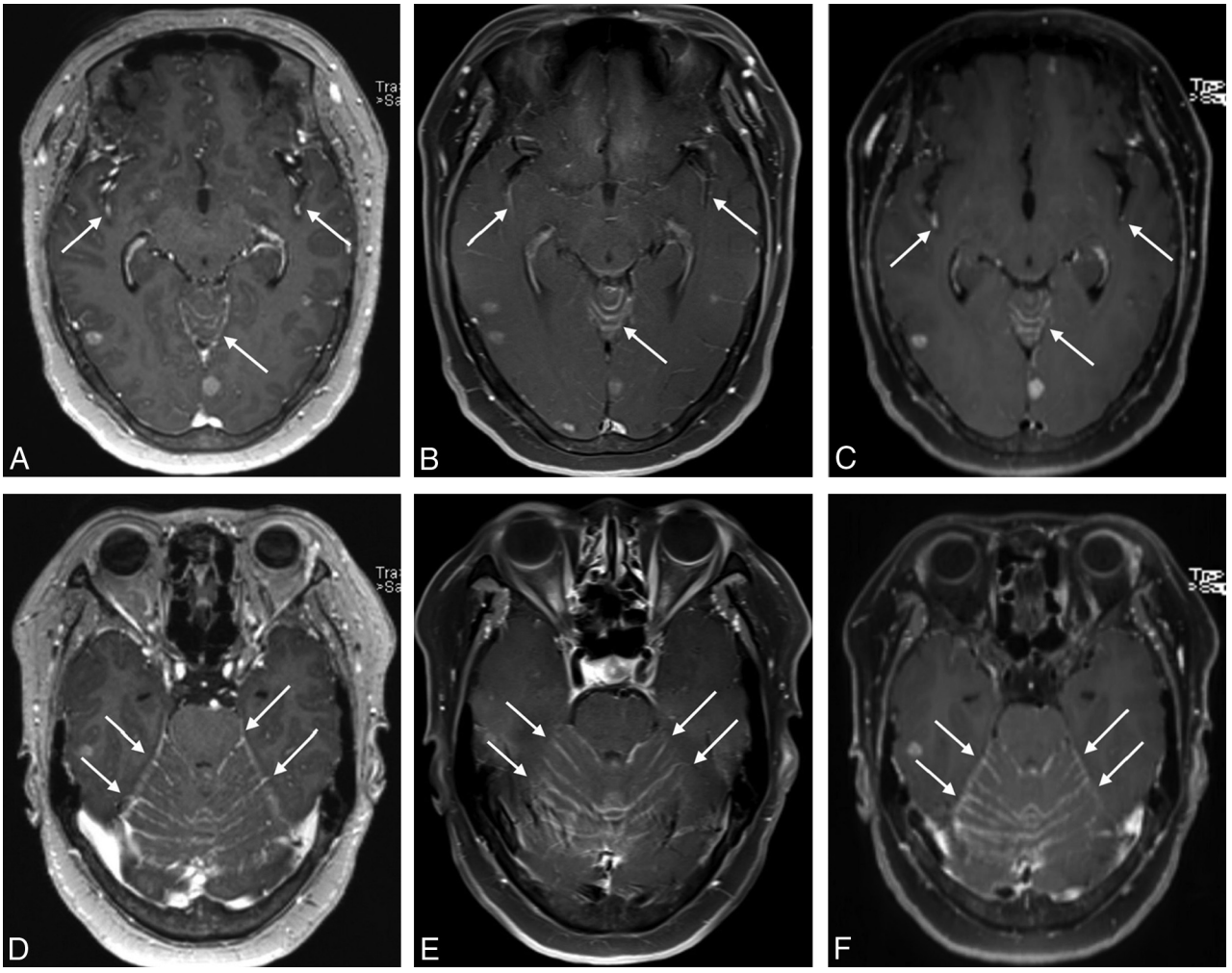

FIG 1. MR images of a 60-year-old female patient with lung cancer. On all contrast-enhanced 3D ultrafast GRE (*A* and *D*), SE T1WI (*B* and *E*), and black-blood imaging (*C* and *F*), leptomeningeal enhancement along the sulci of the bilateral cerebral hemispheres and cerebellar surface was observed (*arrows*).

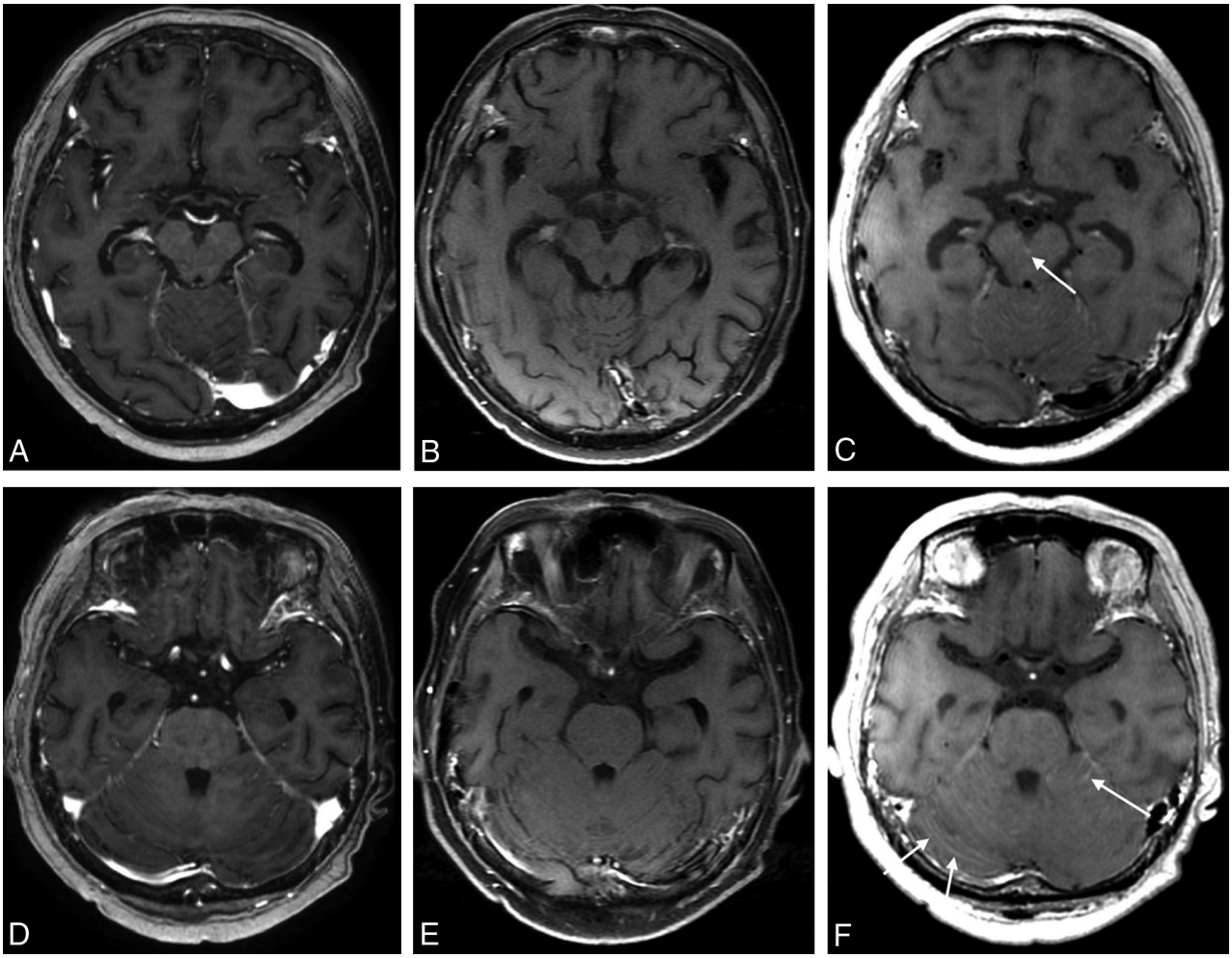

FIG 2. MR images of a 60-year-old female patient with lung cancer. The contrast-enhanced 3D ultrafast GRE (*A* and *D*) and SE T1WI (*B* and *E*) were negatively interpreted by all raters. On only the black-blood imaging (*C* and *F*) scans was leptomeningeal enhancement along the interpeduncular cistern (*C*, *arrow*) and bilateral cerebellar surface observed (*F*, *arrows*).

and subsequent treatment, and the date of last follow-up. The demographic and clinical information is summarized in Table 1.

For all enrolled patients with LC, treatment was performed properly as decided by an oncology team, and tumor progression was tracked at an outpatient clinic with follow-up MR imaging until death or March 2017 if the patient was still alive. Among the 78 patients with LC, 38 patients with lung cancer who underwent at least 1 follow-up MR imaging and had follow-up for at least 3 months if no progression were analyzed with the Kaplan-Meier and the Cox proportional hazards models. Tumor progression was designated as the time when the grade of LC evaluated on the MR imaging was elevated or when the size or number of the primary cancer or metastatic lesions increased. Progression-free survival was defined as the time span from the date of the brain MR imaging to the date of the documented progression or the last clinical follow-up.

Statistical Analysis

The data were checked with the Shapiro-Wilk test for normality and the Levene test for equality of variance. The sensitivity and specificity of the different MR images were calculated, and the Fisher exact test was performed. Additionally, the KPS scores were compared between the groups with different grades using a Mann-Whitney *U* test. To perform the Kaplan-Meier analysis, we dichotomized each parameter regarding the cut-point, which was determined using the method of Contal and O'Quigley,[21] which is based on the log-rank test statistic. For the 38 patients mentioned above, the Kaplan-Meier and the Cox proportional hazards model analyses were performed to determine the relationship between the LC grade evaluated on black-blood imaging and PFS. Additionally, the intraclass correlation coefficient (ICC) was used to assess interobserver agreement. A P value $< .05$ was considered a significant difference. All statistical analyses were performed using commercially dedicated software (MedCalc for Windows, Version 17.6, MedCalc Software, Mariakerke, Belgium; and SPSS 23 software for Windows, IBM, Armonk, New York).

RESULTS

Diagnostic Accuracy of the MR Images

Black-blood imaging (76 of 78 patients with LC, 97.43%) showed a significantly higher sensitivity than CE GRE (50 of 78, 64.1%) and CE SE (52 of 78, 66.67%) for the detection of LC ($P < 0.001$) (Table 2 and Figs 1 and 2). In terms of specificities, we did not find a significant difference among CE GRE (28 of 31 healthy patients,

90.32%), CE SE (28 of 31, 90.32%), and black-blood imaging (30 of 31, 96.77%) ($P > .05$) (Table 3). In addition, the Verio, Achieva dStream, and Discovery MR750w scanners did not show significantly different sensitivities or specificities for CE SE, CE GRE, or black-blood imaging ($P > .05$) (On-line Tables 2 and 3).

LC Grade and KPS

Among 78 patients with LC, only 3 patients (3.9%) had no clinical symptoms at diagnosis. The other 75 patients had neurologic symptoms at the time of diagnosis, and 38 patients (48.7%) had symptoms or signs referable to 1 compartment of the CNS (brain, cranial nerve, or spinal cord), whereas 37 patients (47.4%) had symptoms or signs referable to multiple levels of the neuraxis. Headache, altered mentality, nausea/vomiting, gait difficulty, leg weakness, diplopia, and facial palsy were the most common findings. There was no significant correlation between the presence of each symptom and the LC grade ($P > .05$). In addition, the patients with an LC grade of 5 based on the black-blood imaging had significantly lower KPS scores than the patients with LC grades of 0–4 ($P < .001$) (On-line Table 4).

Relationship between LC and PFS

For the 38 patients with lung cancer, the mean follow-up was 4.64 ± 4.48 months. Among them, 26 (68.4%) patients showed disease progression during the follow-up period. The LC grade evaluated on the follow-up MR imaging was elevated in 7 of the 26 patients (26.9%), the size or number of the primary cancer increased in 8 of the 26 patients (30.8%), and the size or number of the metastatic lesions increased in 11 of the 26 patents (42.3%). The median PFS of the patients was 4.17 months (95% CI, 3.10–6.17 months). The estimated 1-year PFS rate was 26.1%. Table 4 summarizes the results of the Kaplan-Meier analysis for PFS. The Kaplan-Meier analysis identified the time to metastasis (median PFS time, 12.27 versus 3.50 months; $P = .036$), KPS (median PFS time, 11.63 versus 3.37 months; $P = .036$), and a combination of the LC grade and pattern (median PFS time, 4.87 versus 1.77 months; $P = .009$) as significant markers of PFS (Fig 3). Additionally, a Cox proportional hazards model identified a shorter time to metastasis (hazard ratio, 0.25; 95% confidence interval, 0.09–0.71; $P = .009$), a lower KPS (hazard ratio, 0.33; 95% Cl, 0.12–0.89; $P = .029$), and a combined LC grade with a linear pattern (hazard ratio, 2.77; 95% Cl, 1.08–7.08; $P = .034$) as separate independent predictors of PFS (On-line Table 5).

Table 3: Results of the MR imaging readings for cases negative for LC ($n = 31$)

	Imaging Technique		
Findings	CE GRE	CE SE	Black-Blood Imaging
Positive	0	0	0
Indeterminate	3	3	1
Negative	28	28	30
Specificity (%)	90.32	90.32	96.77

Interobserver Agreement

In terms of the interobserver agreements measured, black-blood imaging (0.9636; 95% CI, 0.9516–0.9734) revealed a slightly higher ICC than CE GRE (0.9626; 95% CI, 0.9502–0.9727) and CE SE (0.9342; 95% CI, 0.9124–0.9519) for assessing the grade of the LC (On-line Table 6). In addition, when assessing separately for the presence of LC in each location of cerebral hemispheres, black-blood imaging (range, 0.9017–0.9468) revealed a slightly higher ICC than CE GRE (range, 0.8710–0.9337) and CE SE (range, 0.8665–0.9275) for all locations of the cerebral hemispheres (On-line Table 7).

DISCUSSION

Our study demonstrates that black-blood imaging could improve the diagnostic accuracy for LC, especially for sensitivity, compared with CE GRE and CE SE and that it also has higher interobserver agreement. The grade of LC evaluated on the black-blood imaging showed significant associations with KPS scores. In addition, multivariate analysis using a Cox proportional hazards model revealed that the grade of LC evaluated on black-blood imaging is a significant predictor of PFS when combined with the LC enhancement pattern. On the basis of our study results, we believe that black-blood imaging could complement the low sensitivity of CSF cytology and provide a significant marker of PFS in patients with LC.

To date, several studies have compared the diagnostic accuracy of different MR images in detecting LC. Until now, the sensitivity of MR imaging to LC has been variably known from 20% to 71%.[7,22-24] Singh et al[24] compared the sensitivity of 2D-FLAIR and CE T1-weighted SE in patients with cytologically confirmed LC, and the result was 34% in FLAIR and 66% in CE T1-weighted SE. A subsequent study by Singh et al[15] showed that the sensitivity

Table 4: Kaplan-Meier analysis of the imaging and clinical parameters of PFS ($n = 38$)

		Median Survival (mo) (95% CI)		
Parameters	Threshold Values	Above Threshold or Presence	Below Threshold or Absence	*P* Value
Age (yr)	>60	33.47 (1.77–12.27)	4.57 (3.37–11.63)	.958
Sex		F 3.37 (1.37–4.73)	M 6.17 (3.47–12.27)	.100
Time to metastasis	≤229	12.27 (3.37–15.00)	3.50 (2.53–4.73)	.036
KPS	≤60	11.63 (3.67–13.57)	3.37 (1.37–4.73)	.036
Presence of brain metastasis		3.50 (3.00–4.97)	12.27 (4.57–15.88)	.275
No. of brain metastases	>4	3.47 (1.77–11.63)	4.73 (3.67–12.27)	.701
Presence of extracranial metastasis		3.47 (2.20–11.63)	4.57 (3.37–13.57)	.227
Presence of hydrocephalus		3.47 (2.57–5.37)	4.57 (3.10–6.17)	.607
LC grade		3.47 (1.13–4.97)	4.87 (3.67–12.27)	.449
Enhancement pattern		L 4.17 (2.20–6.17)	N 4.97 (3.00–15.00)	.279
Combination of LC grade and pattern		1.77 (1.07–3.50)	4.87 (3.47–12.27)	.009

Note:—F indicated female patients; M, male patients; L, indicates linear enhancement pattern; N, nodular enhancement pattern.

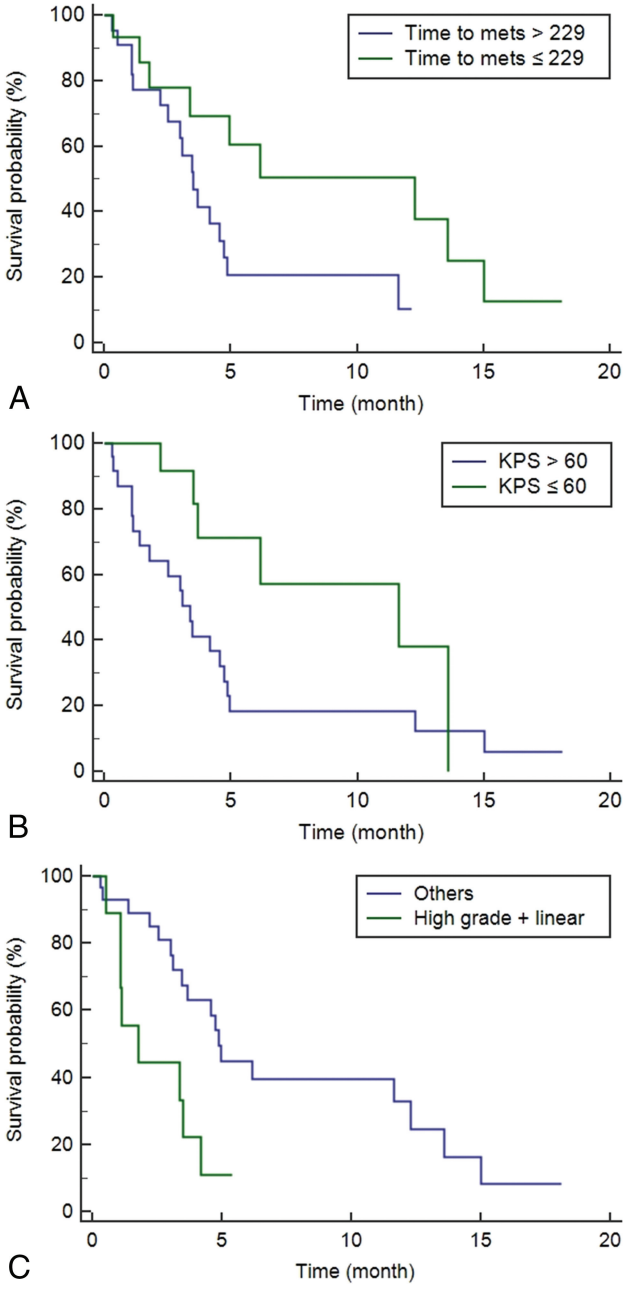

FIG 3. Kaplan-Meier curves showing a significant difference in the progression-free survival for the time to metastasis (*A*), Karnofsky Performance Scale (*B*), and a combination of the LC grade and pattern (*C*) with *P* values of .036, .036, and .009, respectively. When we compared the patients according to the cutoff values, the median PFS times were as follows: 12.27 months (95% CI, 3.37–15.00 months) versus 3.50 months (95% CI, 2.53–4.73 months; $P = .036$) in time to metastasis; 11.63 months (95% CI, 3.67–13.57 months) versus 3.37 months (95% CI, 1.37–4.73 months; $P = .036$) in KPS; and 4.87 months (95% CI, 3.47–1.27 months) versus 1.77 months (95% CI, 1.07–3.50 months; $P = .009$) in a combination of the LC grade and pattern, respectively.

and specificity of CE FLAIR for detecting LC were 41% and 88%, while those of CE T1-weighted MR imaging were 59% and 93%, respectively. LC diagnosis using contrast-enhanced MR imaging has relatively high specificity but still has low sensitivity.

A recently introduced black-blood imaging sequence is one of the 3D SE sequences that nullifies signals from moving flows, in other words, the signal of blood flow. Several studies have demonstrated that black-blood imaging can improve the diagnostic accuracy of small brain parenchymal metastasis due to its higher contrast-to-noise ratio, compared with CE 3D ultrafast GRE and SE T1WI.[13,14] This finding has theoretically been supported by several studies that demonstrated that lesions in CE 3D ultrafast GRE sequences are less enhanced by gadolinium than in SE-based sequences.[11,25] In addition, a recent study comparing 2D-FLAIR, 2D-CE T1-weighted GRE, and black-blood imaging in the diagnosis of LC demonstrated that black-blood imaging showed a better detection rate of LC, regardless of the degree of the rater's experience.[26]

Our study results were in good agreement with previous clinical studies, but our study differs from the previously published studies in some respects. First, we used clear inclusion criteria for those with LC and healthy patients. We only included pathologically or clinically proved patients with LC with a sufficient follow-up period. In addition, we considered LC absent if there was no clinical evidence of LC for a sufficient follow-up after MR imaging (>12 months). Second, we evaluated not only the diagnostic accuracy but also whether the grade of LC evaluated on black-blood imaging was a significant predictor of the patient's KPS scores and PFS. In our study, multivariate analysis showed that the grade of LC evaluated on black-blood imaging is a significant predictor of PFS when combined with the LC enhancement pattern. Therefore, the use of combination of the LC grade and pattern as prognostic biomarkers could improve the stratification of patients with LC at risk of progression and may allow modification of surveillance strategies for specific subgroups who are at high risk of progression. Early diagnosis and proper treatment of progression are the most important strategies for improving overall survival and preventing the deterioration of neurologic symptoms that impair the patient's quality of life. Third, we conducted an analysis of the interobserver agreement, and black-blood imaging was revealed to have a slightly higher ICC than the other sequences for all locations of the cerebral hemispheres, including the cranial nerves. Fourth, our results revealed that there was no significant difference in the diagnostic accuracy of black-blood imaging among the Verio, Achieva dStream, and Discovery MR750w scanners.

There were, however, several limitations in this study. First, this was a retrospective, single-center-based study with some potential bias. In addition, the sample size was rather small because we included only the patients with pathologically confirmed LC or definitive MR imaging findings of LC. Therefore, further studies with a larger number of cases should be performed. Second, unlike previously published studies, the MR imaging examinations were performed with different 3T MR imaging system vendors in this study (Siemens, GE Healthcare, and Philips Healthcare), and this feature may have influenced the overall study results. However, the sensitivity and specificity of each sequence showed no significant differences among the different vendors. Third, in this study, not all conditions of patients were pathologically confirmed. However, we included only patients with a definite sufficient follow-up period in this study. Fourth, our study did not include a postcontrast FLAIR sequence, which is also known to be sensitive to LC. Our hospital obtained black-blood imaging to better detect small metastases or LC in patients with

cancer but did not routinely obtain a postcontrast FLAIR image due to the limitation of scan time. Therefore, further study for the comparison with postcontrast FLAIR is warranted. Finally, in our study, each MR imaging scanning session included CE GRE, CE SE, and black-blood imaging, sequentially. Several studies have suggested that not only on the postcontrast scans performed at an early stage after administration of contrast medium but also on later images, contrast still is sufficient to obtain images of the tumor.[27,28] In addition, a previous study suggested that imaging time delay did not have an effect on lesion conspicuity.[29] However, the scan time after contrast administration may cause some timing bias, so further study that randomizes the order of postcontrast sequences is warranted.

CONCLUSIONS

Black-blood imaging could improve the diagnostic accuracy for LC, especially in sensitivity, compared with CE GRE and CE SE, and it also has a higher interobserver agreement. In addition, a combination of the LC grade and pattern could be an independent predictor of PFS in patients with LC. Therefore, we believe that black-blood imaging is a clinically useful sequence that can play an important role in the early diagnosis as well as the prognosis prediction of patients with LC.

Disclosures: Seung Hong Choi—*RELATED*: *Grant*: governmental grants.* *Money paid to the institution.

REFERENCES

1. Bruna J, González L, Miró J, et al; Neuro-Oncology Unit of the Institute of Biomedical Investigation of Bellvitge. **Leptomeningeal carcinomatosis: prognostic implications of clinical and cerebrospinal fluid features.** *Cancer* 2009;115:381–89 CrossRef Medline
2. Chamberlain MC. **Neoplastic meningitis.** *Neurologist* 2006;12:179–87 CrossRef Medline
3. Park JH, Kim YJ, Lee JO, et al. **Clinical outcomes of leptomeningeal metastasis in patients with non-small cell lung cancer in the modern chemotherapy era.** *Lung Cancer* 2012;76:387–92 CrossRef Medline
4. Nakagawa H, Murasawa A, Kubo S, et al. **Diagnosis and treatment of patients with meningeal carcinomatosis.** *J Neurooncol* 1992;13:81–89 Medline
5. Shapiro WR, Johanson CE, Boogerd W. **Treatment modalities for leptomeningeal metastases.** *Semin Oncol* 2008;36:S46–54 Medline
6. Kaplan JG, DeSouza TG, Farkash A, et al. **Leptomeningeal metastases: comparison of clinical features and laboratory data of solid tumors, lymphomas and leukemias.** *J Neurooncol* 1990;9:225–29 CrossRef Medline
7. Taillibert S, Laigle-Donadey F, Chodkiewicz C, et al. **Leptomeningeal metastases from solid malignancy: a review.** *J Neurooncol* 2005;75:85–99 CrossRef Medline
8. Wasserstrom WR, Glass JP, Posner JB. **Diagnosis and treatment of leptomeningeal metastases from solid tumors: experience with 90 patients.** *Cancer* 1982;49:759–72 Medline
9. Freilich RJ, Krol G, DeAngelis LM. **Neuroimaging and cerebrospinal fluid cytology in the diagnosis of leptomeningeal metastasis.** *Ann Neurol* 1995;38:51–57 CrossRef Medline
10. Clarke JL, Perez HR, Jacks LM, et al. **Leptomeningeal metastases in the MRI era.** *Neurology* 2010;74:1449–54 CrossRef Medline
11. Brant-Zawadzki M, Gillan GD, Nitz WR. **MP RAGE: a three-dimensional, T1-weighted, gradient-echo sequence—initial experience in the brain.** *Radiology* 1992;182:769–75 CrossRef Medline
12. Qiao Y, Steinman DA, Qin Q, et al. **Intracranial arterial wall imaging using three-dimensional high isotropic resolution black blood MRI at 3.0 Tesla.** *J Magn Reson Imaging* 2011;34:22–30 CrossRef Medline
13. Kato Y, Higano S, Tamura H, et al. **Usefulness of contrast-enhanced T1-weighted sampling perfection with application-optimized contrasts by using different flip angle evolutions in detection of small brain metastasis at 3T MR imaging: comparison with magnetization-prepared rapid acquisition of gradient echo imaging.** *AJNR Am J Neuroradiol* 2009;30:923–29 CrossRef Medline
14. Park J, Kim EY. **Contrast-enhanced, three-dimensional, whole-brain, black-blood imaging: application to small brain metastases.** *Magn Reson Med* 2010;63:553–61 CrossRef Medline
15. Singh SK, Leeds NE, Ginsberg LE. **MR imaging of leptomeningeal metastases: comparison of three sequences.** *AJNR Am J Neuroradiol* 2002;23:817–21 Medline
16. Hyun JW, Jeong IH, Joung A, et al. **Leptomeningeal metastasis: clinical experience of 519 cases.** *Eur J Cancer* 2016;56:107–14 CrossRef Medline
17. Kak M, Nanda R, Ramsdale EE, et al. **Treatment of leptomeningeal carcinomatosis: current challenges and future opportunities.** *J Clin Neurosci* 2015;22:632–37 CrossRef Medline
18. Li YS, Jiang BY, Yang JJ, et al. **Leptomeningeal metastases in patients with NSCLC with EGFR mutations.** *J Thorac Oncol* 2016;11:1962–69 CrossRef Medline
19. An YJ, Cho HR, Kim TM, et al. **An NMR metabolomics approach for the diagnosis of leptomeningeal carcinomatosis in lung adenocarcinoma cancer patients.** *Int J Cancer* 2015;136:162–71 CrossRef Medline
20. Mack F, Baumert B, Schäfer N, et al. **Therapy of leptomeningeal metastasis in solid tumors.** *Cancer Treat Rev* 2016;43:83–91 CrossRef Medline
21. Contal C, O'Quigley J. **An application of changepoint methods in studying the effect of age on survival in breast cancer.** *Computational Statistics & Data Analysis* 1999;30:253–70
22. Davis P, Friedman N, Fry S, et al. **Leptomeningeal metastasis: MR imaging.** *Radiology* 1987;163:449–54 CrossRef Medline
23. Chamberlain MC, Sandy AD, Press GA. **Leptomeningeal metastasis: a comparison of gadolinium-enhanced MR and contrast-enhanced CT of the brain.** *Neurology* 1990;40:435–38 CrossRef Medline
24. Singh SK, Agris JM, Leeds NE, et al. **Intracranial leptomeningeal metastases: comparison of depiction at FLAIR and contrast-enhanced MR imaging.** *Radiology* 2000;217:50–53 CrossRef Medline
25. Mugler JP 3rd, Brookeman JR. **Theoretical analysis of gadopentetate dimeglumine enhancement in T1-weighted imaging of the brain: comparison of two-dimensional spin-echo and three-dimensional gradient-echo sequences.** *J Magn Reson Imaging* 1993;3:761–69 CrossRef Medline
26. Gil B, Hwang EJ, Lee S, et al. **Detection of leptomeningeal metastasis by contrast-enhanced 3D T1-SPACE: comparison with 2D FLAIR and contrast-enhanced 2D T1-weighted images.** *PLoS One* 2016;11:e0163081 CrossRef Medline
27. Åkeson P, Nordström CH, Holtås S. **Time-dependency in brain lesion enhancement with gadodiamide injection.** *Acta Radiol* 1997;38:19–24 Medline
28. Schörner W, Laniado M, Niendorf H, et al. **Time-dependent changes in image contrast in brain tumors after gadolinium-DTPA.** *AJNR Am J Neuroradiol* 1986;7:1013–20 Medline
29. Jeon JY, Choi JW, Roh HG, et al. **Effect of imaging time in the magnetic resonance detection of intracerebral metastases using single dose gadobutrol.** *Korean J Radiol* 2014;15:145–50 CrossRef Medline